The Journal of Chemical Physics

RAPID COMMUNICATION | SEPTEMBER 23 2024

Short-time self-diffusion in binary colloidal suspensions

V. Ruzzi ; S. Buzzaccaro ; P. Moretti ; R. Piazza

J. Chem. Phys. 161, 121102 (2024)
https://doi.org/10.1063/5.0225840

AIP Publishing

The Journal of Chemical Physics | COMMUNICATION | pubs.aip.org/aip/jcp

Short-time self-diffusion in binary colloidal suspensions

Cite as: J. Chem. Phys. 161, 121102 (2024); doi: 10.1063/5.0225840
Submitted: 27 June 2024 • Accepted: 5 September 2024 •
Published Online: 23 September 2024

V. Ruzzi,[a] S. Buzzaccaro,[b] P. Moretti, and R. Piazza

AFFILIATIONS

Department of Chemistry, Materials Science, and Chemical Engineering (CMIC), Politecnico di Milano, Edificio 6, Piazza Leonardo da Vinci 32, 20133 Milano, Italy

[a]**Present Address:** Laboratoire Charles Coulomb (L2C), Université Montpellier, CNRS, Montpellier, France.
[b]**Author to whom correspondence should be addressed:** stefano.buzzaccaro@polimi.it

ABSTRACT

The Brownian dynamics of a colloidal particle is consistently modified by the presence in the solvent of other particles of comparable size, whose effects on the particle diffusion coefficient cannot be attributed to a change of the effective solvent viscosity. So far, despite their impact on subjects ranging from microrheology to phoretic transport in crowded environments, a detailed experimental survey of these effects is still lacking. By exploiting the peculiar properties of fluorinated colloidal particle, we have performed an extensive dynamic light scattering (DLS) investigation of short-time self-diffusion in binary colloidal mixtures, focusing on systems where one of the two species (the "tracer" particles) is very diluted compared to the other one (the "host" particles). From the dependence on the host concentration of the DLS correlation function, we have obtained the first-order correction h^s_{s1} to the tracer single-particle diffusion coefficient, varying the tracer-to-host size ratio q in the range $0.2 \le q \le 2$. Our results support the functional relation of h^s_{s1} on q proposed to account for the theoretical and numerical results for hard-sphere mixtures. However, h^s_{s1} seems to have a weaker dependence on the size ratio than theoretically predicted, possibly because of an imperfect matching of the suspensions we used for an ideal hard-sphere mixture. This may be due to the presence of a stabilizing surfactant layer on the particle surface that, although very thin, has significant effects on hydrodynamic lubrication forces.

I. INTRODUCTION

The Brownian motion of colloidal particles in complex, structured solvents is a subject of primary interest because of its relation with diffusion in crowded environments, such as the cell interior,[1–7] and for its connection with both passive and active microrheology[8–10] or particle manipulations in non-Newtonian fluids.[11] Unfortunately, this is also a very challenging subject, both theoretically and numerically, even in the simplest case of the diffusion of a tracer spherical particle of radius a_T in a colloidal dispersion of host hard spheres (HS) with a different radius a_H, primarily because of the many-body nature of the interparticle hydrodynamic interactions (HI). A further complication is that the self (tracer) diffusion coefficient D_s is time dependent because if the host suspension is not very diluted, the particle mean square displacement is not linear in time, so one should distinguish between a short and a long time limit for D_s.

Two limits are, however, easily spotted. Indeed, when the host particles are very small compared to the tracer, i.e., when the size ratio $q = a_T/a_H$ is very large,[12] we can reasonably assume that their effect is just modifying the bare solvent viscosity η_0 according to the Einstein formula,[13,14]

$$\eta_{eff} = \eta_0(1 + 2.5\phi),$$

where ϕ is the particle volume fraction of the host dispersion.

At first order in ϕ, therefore, the tracer self-diffusion coefficient becomes

$$D_s(\phi) = D_0(1 - 2.5\phi),$$

where $D_0 = k_B T/6\pi\eta_0$. In the opposite limit $q \ll 1$, the host particles can be viewed as a macroscopic porous (and nearly static) medium with huge cavities, allowing for a unhindered diffusion of the tracer with $D_s(\phi) = D_0$. For an arbitrary value of q and in the short time limit, we can expand the tracer diffusion coefficient D_s^s as

$$D_s^s(\phi;q) = D_0 H_s^s(\phi;q) = D_0(1 - h_{s1}^s(q)\phi + h_{s2}^s(q)\phi^2 + \cdots).$$

When the tracer and host particles have the same size ($q = 1$), accurate calculations,[15] accounting for lubrication forces to prevent divergent three-particle HI contributions, yield, at second order in ϕ,

$$H_s^s(\phi; q = 1) = 1 - 1.832\phi - 0.219\phi^2. \quad (1)$$

However, this theoretical value for $h_{s2}^s(q)$strikingly disagrees (even in sign) with the experimental evidence[16,17] that rather supports the semi-empirical expression proposed by Lionberger and Russel,[18]

$$H_s^s(\phi; q = 1) \simeq (1 - 1.56\phi)(1 - 0.27\phi), \quad (2)$$

which vanishes (as it should) at random close packing $\phi_{rcp} \simeq 0.64$ and at the same order reads

$$H_s^s(\phi; q = 1) = 1 - 1.83\phi + 0.42\phi^2. \quad (3)$$

For an arbitrary value of q, the problem is even more complicated and was solved only to first order in ϕ by Batchelor and co-workers, assuming indeed pair HI.[19–22] With a true mathematical *tour de force*, they obtained

$$h_{s1}^s(q) = \left(\frac{1+q}{2}\right)^3 C(q), \quad (4)$$

where $C(q)$ is numerically obtained as the integral of an expression that intricately depends on the interparticle distance and mobilities.[23]

Experimental investigations are certainly not less challenging. For single-component dispersions, the standard way to obtain D_s^s is by using dynamic light scattering (DLS) for measuring the large wave-vector limit of the intermediate structure factor $S(k,t)$,[16,24] which provides information on the single-particle motion over a distance $d \simeq 2\pi/k$ that, to ensure that direct interparticle forces do not affect diffusion, has to be much smaller than the mean interparticle distance. Achieving this condition with DLS may, however, be difficult since the maximum accessible wave-vector is $k_{\max} = 4\pi/\lambda$, where λ is the light wavelength in the scattering medium. Dense suspensions of small particles are then better studied with x-ray photon correlation spectroscopy (XPCS).[25,26] An interesting alternative approach is using optically anisotropic particles dispersed in an index-matching solvent. Optical matching suppresses the coherent polarized contribution to the scattered intensity, leaving only a depolarized, incoherent component whose correlation function has a decay rate $D_r + D_s^s k^2$, where D_r is the particle rotational diffusion coefficient.[27] This experimental approach has provided accurate measurements of D_s^s up and above the HS freezing volume fraction $\phi \simeq 0.5$.[17]

With particle mixtures, one could, in principle, make particle-tracking experiments, which are, however, best suited to study two-dimensional diffusion and can hardly measure displacements much smaller than the particle size, unless they are performed with a holographic microscope. Indeed, the only comprehensive investigation done by particle tracking of diffusion in a binary colloidal mixture that we are aware of is limited to a single value of the size ratio q.[28] Using particles with a different refractive index in an optically matched host suspension is almost unavoidable in order to use DLS. Optical matching is commonly achieved by using poly(methylmethacrylate) (PMMA) particles in a suitable decalin–tetralin mixture. However, the difference in refractive index between PMMA and other colloidal particles stable in an organic solvent, such as silica,[29] is rather small. Thus, extreme care should be taken to avoid optical polydispersity effects that would prevent fully masking of the host particles, especially if $a_H \gg a_T$. As a result, DLS studies of self-diffusion exploiting this approach are mostly limited to suspensions of tracers and hosts with a very similar size ($q \simeq 1$).[30–32] Using low refractive index host particles that can be optically matched in water opens much wider experimental possibilities. In this work, by using monodisperse particles made of a highly fluorinated hydrocarbon, we show that the range $0.2 \lesssim q \lesssim 2$ can be fully covered, allowing a detailed comparison with existing theories of self-diffusion in binary colloidal mixtures.

TABLE I. Tracer particles size properties. σ_{rel} is the relative standard deviation or coefficient of variation.

Nos.	Material	a_T (nm)	σ_{rel} (%)	q
1	PS	30	2.0	**0.20**
2	PS	42	2.0	**0.28**
3	PMMA	53	4.8	**0.35**
4	PMMA	98	2.0	**0.65**
5	PMMA	143	2.4	**0.95**
6	PMMA	224	2.2	**1.49**
7	PMMA	300	2.2	**2.00**

II. EXPERIMENTAL

A. Colloidal system

Fluorinated nanoparticles, hereinafter referred to as FMA, have been synthesized via heterogeneous emulsion free-radical polymerization, following the method described in Refs. 33 and 34, using as monomer 2,2,3,3,4,4,4-heptafluorobutyl methacrylate (HFBMA, Alfa Aesar), surfactant sodium dodecyl sulfate (SDS) as emulsifier, and potassium persulfate as initiator, purchased from Sigma-Aldrich. The suspension, with a solid content of about 1% obtained from the batch reaction, was further purified by dialysis carried on for eight days. The particles were then stabilized with Triton X-100, a non-ionic surfactant that physically adsorbs on FMA particles as a 2 nm monolayer ensuring the stability of the dispersion up to an ionic strength of 0.5M.

PMMA particles and PS particles, used as guest tracers, are purchased from microParticles GmbH and PolyScience, respectively. The nominal radius a_T, relative standard deviation σ_{rel}, and size ratio q are presented in Table I.

B. Particle characterization and sample preparation

1. Density

The density of colloidal particles is typically obtained from the values of the settling speed in an analytical centrifuge using Stokes' law, which as an input, however, requires precise values for the particle size and for the solvent viscosity. To improve the accuracy, we followed a different method. Using aqueous mixtures of sodium polytungstate, a multivalent salt known to be miscible with water, we prepared a series of solvents with a density ranging from 1.0 to 3.1 g/cm^3. The particle density was then obtained by adjusting the solvent composition until settling or creaming under centrifugation was negligible,[35] which yielded a density of the FMA particles $\rho_{\text{FMA}} \simeq 1.578 \pm 0.005$ g/cm^3. Such a precise value of the particle density also allows an accurate value of the particle volume fraction ϕ of the FMA samples we used, which is obtained as

$$\rho = \rho_s + \phi(\rho_{\text{FMA}} - \rho_s), \tag{5}$$

where ρ and ρ_s are the suspension and the solvent densities, respectively.

2. Particle size

The particle average size and polydispersity were obtained using a custom angular DLS setup with a frequency-doubled Nd:Yag laser operating at $\lambda = 532$ nm. All the measurements were performed at $T = 20 \pm 0.1\,^\circ$C. A second cumulant fit of the field correlation function from a dilute sample ($\phi \simeq 10^{-4}$) at a scattering angle $\theta = 90^\circ$, shown in the inset of Fig. 1(a), yields a particle radius $a_H = (150 \pm 3)$ nm.

3. Refractive index

By measuring as a function of the solvent refractive index, varied by mixing water with urea, the intensity I of the light scattered at 90° from a dilute particle suspension allowed us to obtain a very accurate value of the FMA particle refractive index. The experimental values of the excess scattering intensity $I - I_s$ normalized with

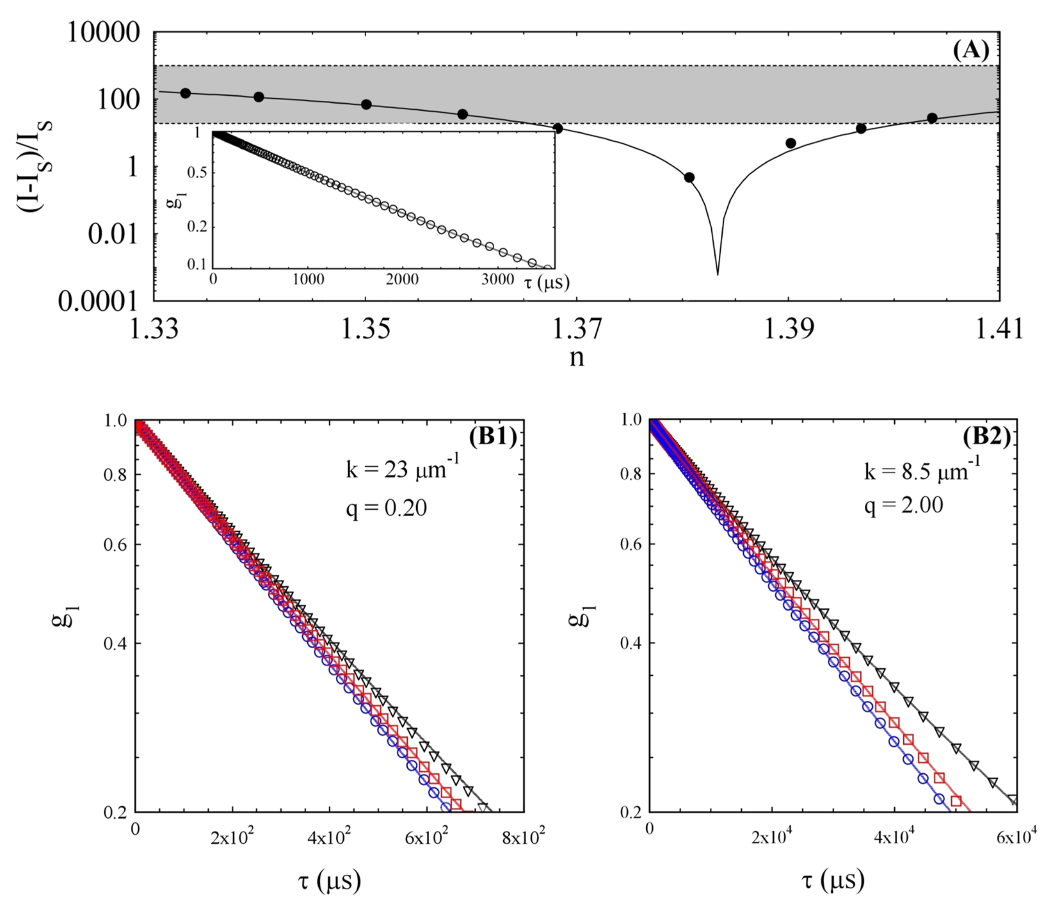

FIG. 1. Panel (a): semilogarithmic plot of the normalized excess scattered intensity $(I - I_s)/I_s$ at $\theta = 90^\circ$ from an FMA suspension as a function of the solvent refractive index. The continuous line is a parabolic fit with a minimum at $n = 1.383$. For all the samples we investigated, the values of the intensity scattered by tracers lie within the gray region. The inset shows, on a logarithmic y axis, a field correlation function for a dilute FMA suspension. Panels (b): field correlation functions of the tracer particles for $q = 0.20$ (b1) and $q = 2.00$ (b2) at three different host volume fractions: $\phi = 0.01$ (circles), $\phi = 0.04$ (squares), and $\phi = 0.085$ (triangles), obtained at scattering wave-vectors indicated in the graphs. The continuous lines are two cumulants fits to the correlation functions, $g_1(\tau) = \exp(-\Gamma\tau + (1/2)\Gamma_2\tau^2)$.

respect to the solvent scattered intensity I_s, which is a quadratic function of the solvent refractive index,[36] are shown in Fig. 1(a). The minimum of the parabola yields an average refractive index of Triton-coated FMA of $\bar{n}_{\text{FMA}} = 1.383 \pm 0.001$.

4. Sample preparation

The initial FMA batch is first concentrated by centrifugation to a volume fraction $\phi = 0.154$ in water. NaCl is then dissolved to a final concentration of 20 mM. By adding urea, the suspension is finally optically matched and further centrifuged to get a mother batch concentration $\phi = 0.244 \pm 0.005$. For each size ratio, we prepared and measured seven samples with a volume fraction of the host FMA particles ranging from $\phi = 0.01$ to $\phi = 0.1$.

Suspensions of the tracer particles are prepared in a solvent having the same composition of the FMA mother batch, and their volume fraction ϕ_T is adjusted so as to obtain a scattered intensity from the tracer particles that is at least two orders of magnitude larger than the intensity scattered by the host particles [see Fig. 1(a)]. At any rate, the final volume fraction of the added tracers is kept below $\phi_T \simeq 10^{-3}$ to avoid multiple scattering effects.

After the DLS measurements of the particle mixtures, the samples are centrifuged at 14 000 g for 2 h to separate out the host particles from the solvent. When using PS tracers, the surnatant is pipetted out and transferred again to the scattering cell to obtain the value D_0 of the diffusion coefficient of the pure tracer. PMMA tracers, however, separate out with the host particles, thus a tiny amount of them must be added to the surnatant to get D_0.

III. RESULTS

The field correlation functions obtained for the lowest $(q = 0.20)$ and highest $(q = 2.00)$ size ratios are shown in panels (b1) and (b2) of Fig. 1 for three representative host volume fractions $\phi = 0.01, 0.04, 0.085$.

For $q = 0.2$, the data were obtained at a scattering angle $\theta = 90^\circ$, corresponding to $k \simeq 23\ \mu\text{m}^{-1}$. The field correlation functions display a single-exponential behavior, with only modest deviations that can be attributed to polydispersity effects. The decay rate, obtained from a two-cumulant fit, ranges from $\Gamma \simeq 2.53\ \text{ms}^{-1}$ to $\Gamma \simeq 2.30\ \text{ms}^{-1}$.

It is worth checking that, under these conditions, the measured relaxation times are properly related to self-diffusion in short time regime. We first notice that up to the maximum host volume fraction $\phi = 0.1$ we tested, the average distance between the host particles is $d_H \sim [4\pi/(3\phi)]^{1/3} a_H \le 3.5 a_H$. Then, we have to distinguish the two cases $q \lessgtr 1$. For $q < 1$, the fastest particles are the tracers, thus at time τ, the dynamics is still in the short time regime if the tracers mean square displacement $\langle \Delta r_T^2(\tau)\rangle = -(6/k^2)\ln g_1(\tau) < {d_H}^2$, which is verified at all delay times we measured. For $q > 1$, the fastest particles are the host, whose mean square displacement can be estimated[37] as $\langle \Delta r_H^2(\tau)\rangle = q\langle \Delta r_T^2(\tau)\rangle$. In this case, measurements performed at a scattering angle of 90° are still in the short time regime. However, for $q = 2$, the tracers scatter mainly in the *forward* direction. Therefore, for the scattered intensity of the tracer to be dominant, DLS measurements were performed at $\theta = 30^\circ$ $(k \simeq 8.5\ \mu\text{m}^{-1})$, where the ratio of the host to tracers scattered intensities is about 0.01. At this scattering vector, however, DLS probes the short time dynamics only for $g_1(\tau) > 0.2$. Limiting our fit to this value of τ ensures that the diffusion both of the tracer and the host particles are in the short-time regime, as requested by the theoretical predictions.[21,38]

In this decay range, the field correlation functions still display an almost exponential behavior, but characterized by longer decay times $(\Gamma \simeq 0.0335 - 0.0276\ \text{ms}^{-1})$.

Figure 2 shows the normalized short-time normalized self-diffusion coefficients $H_s^s(\phi;q)$as a function of ϕ for the lowest and highest investigated q values, fitted as $H_s^s(\phi;q) = A(1 - h_{s1}^s(q)\phi)$. The slope of the curves increases with the size ratio, from $h_{s1}^s(0.20) \simeq 1.023 \pm 0.018$ to $h_{s1}^s(2.00) \simeq 2.209 \pm 0.098$. A linear fit to $H_s^s(\phi;q)$for a size ratio $q = 0.95$, which is also shown in the figure, yields $h_{s1}^s(0.95) \simeq 1.754 \pm 0.117$, which is only 4% lower than the theoretically calculated value $h_{s1}^s(1) = 1.83$ for a single-component suspension of HS.

In the inset of Fig. 3, we compare our results for $q = 0.20$ and $q = 2.00$ to the diffusion coefficient predicted by the theory of Zhang and Nägele,[38] who have improved the calculation of $h_{s1}^s(q)$by means of a cluster expansion. The maximum deviation with respect to the theory (black dashed line) never exceeds 3%. However, while for $q = 2.00$ our results are randomly scattered around the theoretical values, for $q = 0.20$ a small but statistically significant deviation from the theory is observed: the measured diffusion coefficients are smaller than expected, with a difference that grows with ϕ.

This discrepancy is better appreciated by plotting $[h_{s1}^s(q)]^{-1}$ vs q^{-1} as in the body of Fig. 3. Following Batchelor,[21] Zhang and Nägele[38] have indeed shown that the q-dependence of the theoretical results for $h_{s1}^s(q)$can be empirically fitted as

$$h_{s1}^s(q) = \frac{2.5}{1 + hq^{-1}}, \tag{6}$$

where the value they find for the only free parameter h $(h = 0.366)$ is pretty similar to the value that Batchelor obtained for the numerical results in Ref. 20 $(h = 0.359)$. Equation (6) then suggests that

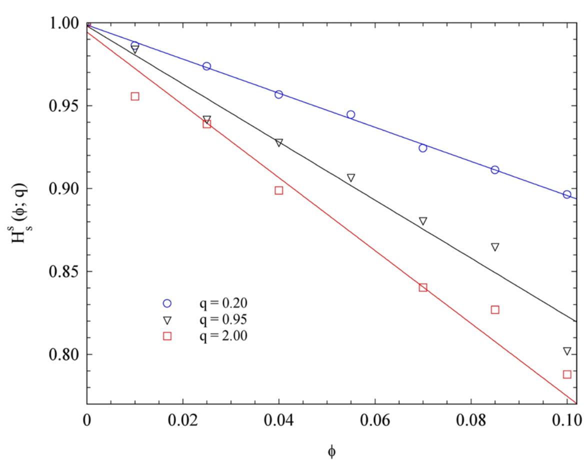

FIG. 2. Normalized short-time self-diffusion coefficients $H_s^s(\phi;q)$for $q = 0.20$ (circles), $q = 0.95$ (triangles), and $q = 2.00$ (squares). The full lines are linear fits of the data points $H_s^s = H_0(1 - h_{s1}^s(q)\phi)$, yielding $h_{s1}^s(q = 0.20) = 1.023 \pm 0.018$, $h_{s1}^s(q = 0.95) = 1.754 \pm 0.117$, and $h_{s1}^s(q = 2.00) = 2.209 \pm 0.098$, respectively.

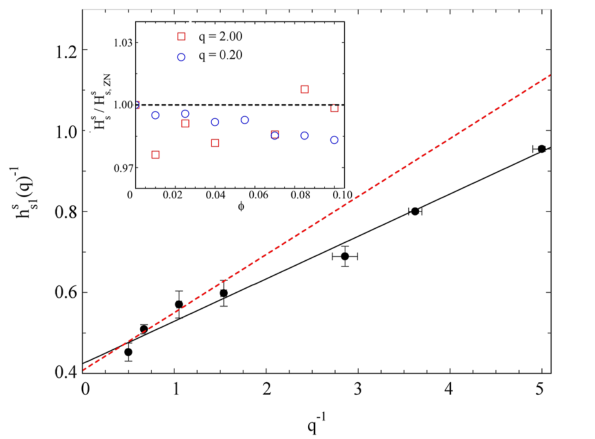

FIG. 3. Plot of $[h_{s1}^s(q)]^{-1}$ vs the reciprocal of the size ratio q. A linear fit to the data (full line), $[h_{s1}^s(q)]^{-1} = a(1 + hq^{-1})$, gives $a = 0.424 \pm 0.013$, corresponding to $\lim_{q\to\infty} h_{s1}^s(q) = 2.36 \pm 0.07$ and $h = 0.247 \pm 0.015$. For comparison, the dashed line shows the theoretical result by Zhang and Nägele. The inset shows, for $q = 0.2$ and $q = 2$, the measured short-time diffusion coefficients scaled to the theoretical results obtained by Zhang and Nägele.[38]

$[h_{s1}^s(q)]^{-1}$ should linearly increase with the inverse size ratio. Figure 3 shows that the experimental data are in reasonable agreement with the linear trend of Eq. (6). However, while the intercept is pretty close to the Einstein value of 2.5, the slope $h \simeq 0.247$ is ~30% lower than the theoretical one.

IV. DISCUSSION AND CONCLUSIONS

The diffusion coefficient of a colloidal particle is consistently influenced by the presence in the solvent of structures on length scales that are not negligible compared to the particle size, an effect that cannot simply be traced back to changes in the solvent rheology. The aim of this work is probing these effects, which have mostly been qualitatively investigated despite their paramount importance in crowded biological environments, on a well-controlled model system. By exploiting the peculiar properties of fluorinated colloidal particles, which can be optically matched in aqueous solvents, we have performed an extensive DLS investigation of short-time self-diffusion in binary colloidal mixtures. We focused on the specific case, where one of the two species (the "tracer") is very diluted compared to the other one (the "host"), increasing the volume fraction ϕ of the host particle up to $\phi = 0.1$ and varying the tracer-to-host size ratio in the range $0.2 \le q \le 2$. From these measurements, we have obtained the correction at first order in ϕ of the tracer short-time diffusion coefficient, $h_{s1}^s(q)$, which we compared to the theoretical predictions.[21,38] We found that the dependence of $h_{s1}^s(q)$on the size ratio agrees with the empirical functional form proposed by Batchelor and Nägele, however, with an experimental value of the coefficient h in Eq. (6) that is consistently lower than the theoretical value.

To account for this discrepancy, we first have to point out that in the system we investigated, both the tracer and the host particles are coated with a surfactant. One may, therefore, wonder whether and how much this stabilizing layer affects diffusion, preventing a straightforward comparison with an ideal HS mixture. Moreover, it should be noted that in sterically stabilized colloidal systems, the values of the particle size and volume fraction that are required for a proper mapping onto an ideal HS system have been the subject of an extensive debate.[39,40] It is indeed a common practice introducing an effective volume fraction ϕ_{eff} and/or an effective radius r_{eff}, so as to match the theoretical expectation for some property of a HS system[39] using either static quantities [Eq. (5) is an example] or transport coefficients, like matching the viscosity of a dilute suspension to the Einstein expression (which is valid whatever the interparticle forces).

In this work, we choose to define r_{eff} as the particle hydrodynamic radius r_h obtained by DLS. Yet, for sterically stabilized particles, two other radii can be defined, namely, a "core" radius r_c and a "core–shell" radius $r_{cs} = r_c + \delta$, where δ is the thickness of the stabilizing layer. However, usually one finds that $r_c \le r_h \le r_{cs}$, so that stating which value of the radius is more appropriate for a comparison with theory is nontrivial and particularly delicate when testing in dynamical properties that crucially depend on hydrodynamic interactions. Indeed, lubrication forces acting when two particles close in contact give a significant contribution to D_s^s.[41] For a pair of ideal hard spheres, the hydrodynamic friction caused by the relative motion of two near-by particle boundaries actually *diverges* when their center-to-center distance is equal to their diameter. However, this singular contribution vanishes for a sterically stabilized sphere at a distance $d = 2r_{eff}$ because of the presence of a narrow permeable channel where the solvent can flow. Therefore, HI can be different between hard non-permeable spheres and core–shell particles with the same hydrodynamic radius, even for extremely thin and only slightly permeable outer shells.[42] These qualitative observations are supported by a nontrivial extension of the effective HS model, the core–shell model, in which the particles are covered by a porous layer of thickness δ and constant permeability $\tilde{k}$.[41] It has been shown that, even when the shell is thin, the dynamical properties of the core–shell particles are poorly approximated by HS of radius r_{cs}.[42] Nevertheless, the dynamics of a concentrated core–shell system is well reproduced if the thin permeable shell is replaced by the shell of a pure fluid,[42] like in the annulus model introduced by Cichocki and Felderhof.[43]

So far, we cannot make a full comparison of our results with the annulus model, which has been solved for the monodisperse case alone. However, for $q = 1$ and $\delta / r_c = 0.05 - 0.1$, the model predicts that $h_{s1}^s(q)$can be 10%–20% larger than for the HS system (see Fig. 4 in Ref. 42), which is consistent with our results. The experimental observation that the deviation from the HS prediction is more pronounced for smaller tracers suggests that the stabilizing layer cannot be neglected to obtain accurate values of their diffusion coefficient. We also point out that under our experimental condition, the Debye–Hückel length is around 2.2 nm, a length comparable to δ, so that electrostatic effects can play an additional role in lubrication forces. The effect of the surface layer on D_s^s can be better quantified by performing experiments where δ, and possibly $\tilde{k}$ too, are varied using different stabilizing surfactants.

Finally, we point out that the host FMA particles we used could be profitably exploited to investigate other transport properties. For instance, the long-time self-diffusion coefficient, which requires taking correlation measurements at a very small scattering wave-vector, can be investigated using digital Fourier imaging.[44–46] Similarly, the sedimentation kinetics in binary suspensions and the onset of hydrodynamic instabilities[47] could be made using Ghost Particle Velocimetry (GPV), a technique requiring to use small "phantom" particles.[48,49] Hence, we are confident that our approach could provide valuable insights into the transport properties of complex binary mixtures.[50]

ACKNOWLEDGMENTS

We thank Filippo Faedi for help in preliminary measurements and Enrico Lattuada for suggestions about the particle synthesis protocol. This research was funded by the Italian Ministry of University and Research (PRIN Project No. 20222MCY75) and by the Italian Space Agency (ASI, Project "NESTEX").

AUTHOR DECLARATIONS

Conflict of Interest

The authors have no conflicts to disclose.

Author Contributions

V. Ruzzi: Data curation (equal); Formal analysis (equal); Investigation (equal); Methodology (equal); Writing – original draft (equal); Writing – review & editing (equal). **S. Buzzaccaro**: Conceptualization (supporting); Data curation (equal); Formal analysis (equal); Funding acquisition (equal); Investigation (equal); Methodology (equal); Supervision (equal); Writing – original draft (equal); Writing – review & editing (equal). **P. Moretti**: Investigation (supporting). **R. Piazza**: Conceptualization (lead); Formal analysis (equal); Funding acquisition (equal); Investigation (equal); Methodology (equal); Project administration (lead); Resources (lead); Supervision (equal); Writing – original draft (equal); Writing – review & editing (equal).

DATA AVAILABILITY

The data that support the findings of this study are available from the corresponding author upon reasonable request.

REFERENCES

[1] T. Ge, Macromolecules **56**, 3809 (2023).
[2] L. Petit, C. Barentin, J. Colombani, C. Ybert, and L. Bocquet, Langmuir **25**, 12048 (2009).
[3] L. Cai, S. Panyukov, and M. Rubinstein, Macromolecules **44**, 7853 (2011).
[4] J. Miao, M. Tsige, and P. Taylor, J. Chem. Phys. **147**, 044904 (2017).
[5] F. Burla, T. Sentjabrskaja, G. Pletikapic, J. van Beugen, and G. Koenderink, Soft Matter **16**, 1366 (2020).
[6] B. Fabry, G. Maksym, J. Butler, M. Glogauer, D. Navajas, and J. Fredberg, Phys. Rev. Lett. **87**, 148102 (2001).
[7] D. Wirtz, Annu. Rev. Biophys. **38**, 301 (2009).
[8] S. Lai, Y. Wang, D. Wirtz, and J. Hanes, Adv. Drug Delivery Rev. **61**, 86 (2009).
[9] T. Waigh, Rep. Prog. Phys. **79**, 074601 (2016).
[10] F. Orts, M. Maier, M. Fuchs, G. Ortega, E. M. Garzón, and A. M. Puertas, J. Chem. Phys. **159**, 144901 (2023).
[11] X. Lu, C. Liu, G. Hu, and X. Xuan, J. Colloid Interface Sci. **500**, 182 (2017).
[12] The actual q-value after which the effective fluid regime is reached depends significantly on the considered diffusion property.[54]
[13] A. Einstein, "Eine neue bestimmung der moleküldimensionen," Ph.D. thesis, ETH Zurich, 1905.
[14] A. Einstein, Ann. Phys. **339**, 591 (1911).
[15] B. Cichocki, M. Ekiel-Jezewskaa, and E. Wajnrybb, J. Chem. Phys. **111**, 3265 (1999).
[16] P. Segre, O. Behrend, and P. Pusey, Phys. Rev. E **52**, 5070 (1995).
[17] V. Degiorgio, R. Piazza, and R. B. Jones, Phys. Rev. E **52**, 2707 (1995).
[18] R. A. Lionberger and W. B. Russel, J. Rheol. **41**, 399 (1997).
[19] G. K. Batchelor, J. Fluid Mech. **74**, 1–29 (1976).
[20] G. K. Batchelor and C.-S. Wen, J. Fluid Mech. **124**, 495–528 (1982).
[21] G. K. Batchelor, J. Fluid Mech. **131**, 155–175 (1983).
[22] G. K. Batchelor, J. Fluid Mech. **137**, 467–469 (1983).
[23] A numerical evaluation of $C(q)$ for a generic q also allowed Batchelor and Wen to obtain settling velocity of a guest particle in a host dispersion.[20] Unfortunately, their calculation of the mobility coefficients, based on previous results by Jeffrey and Onishi[51] were partly wrong. Nevertheless, this do not affect the evaluation of the short-time self diffusivity (see http: ryuon.sourceforge.nettwobodyerrata.html and the corrected derivation in Ref. 52).
[24] W. van Megan, S. M. Underwood, R. H. Ottewill, N. S. J. Williams, and P. N. Pusey, Faraday Discuss. Chem. Soc. **83**, 47 (1987).
[25] D. Lumma, L. Lurio, M. Borthwick, P. Falus, and S. Mochrie, Phys. Rev. E **62**, 8258 (2000).
[26] D. Orsi, A. Fluerasu, A. Moussaïd, F. Zontone, L. Cristofolini, and A. Madsen, Phys. Rev. E **85**, 011402 (2012).
[27] V. Degiorgio, R. Piazza, and T. Bellini, Adv. Colloid Interface Sci. **48**, 61 (1994).
[28] A. L. Thorneywork, D. G. Aarts, J. Horbach, and R. P. Dullens, Phys. Rev. E **95**, 012614 (2017).
[29] Melamin (MF) resin particles have a refractive index n = 1.68, which is quite higher than PMMA (n = 1.48). However, monodisperse MF particles have been available only recently and in a limited size range.
[30] W. van Megen, S. Underwood, and I. Snook, J. Chem. Phys. **85**, 4065 (1986).
[31] W. van Megen and S. Underwood, J. Chem. Phys. **91**, 552 (1989).
[32] For what concerns the *rotational* dynamics, the self diffusion for three different q values was studied using a combination of depolarized dynamic light scattering (DDLS) and time-resolved phosphorescence anisotropy (TPA).[53]
[33] G. H. Koenderink, S. Sacanna, C. Pathmamanoharan, M. Raşa, and A. P. Philipse, Langmuir **17**, 6086 (2001).
[34] M. Zupkauskas, Y. Lan, D. Joshi, Z. Ruff, and E. Eiser, Chem. Sci. **8**, 5559 (2017).
[35] U. Capasso Palmiero, A. Agostini, E. Lattuada, S. Gatti, J. Singh, C. T. Canova, S. Buzzaccaro, and D. Moscatelli, Soft Matter **13**, 6439 (2017).
[36] R. Piazza and V. Degiorgio, Opt. Commun. **92**, 45 (1992).
[37] This relation is exact for $\phi \to 0$ and is an upper limit for $\phi \neq 0$.
[38] H. Zhang and G. Nägele, J. Chem. Phys. **117**, 5908 (2002).
[39] W. Poon, E. Weeks, and C. Royall, Soft Matter **8**, 21 (2012).
[40] C. Royall, W. Poon, and E. Weeks, Soft Matter **9**, 17 (2013).
[41] G. Abade, B. Cichocki, M. Ekiel-Jezewska, G. Nägele, and E. Wajnryb, J. Chem. Phys. **136**, 104902 (2012).
[42] B. Cichocki, M. Ekiel-Jezewska, and E. Wajnryb, Colloids Surf., A **418**, 22 (2013).
[43] B. Cichocki and U. Felderhof, J. Chem. Phys. **94**, 556 (1991).
[44] R. Cerbino and V. Trappe, Phys. Rev. Lett. **100**, 188102 (2008).
[45] F. Giavazzi and R. Cerbino, J. Opt. **16**, 083001 (2014).
[46] S. Buzzaccaro, M. Alaimo, E. Secchi, and R. Piazza, J. Phys.: Condens. Matter **27**, 194120 (2015).
[47] R. Piazza, Rep. Prog. Phys. **77**, 056602 (2014).

[48] S. Buzzaccaro, E. Secchi, and R. Piazza, Phys. Rev. Lett. **111**, 048101 (2013).
[49] E. Lattuada, "Experimental study of the sedimentation of complex colloidal suspensions," Ph.D. thesis, Politecnico di Milano, 2019.
[50] C. Beck, M. Grimaldo, H. Lopez, S. Da Vela, B. Sohmen, F. Zhang, M. Oettel, J. Barrat, F. Roosen-Runge, F. Schreiber, and T. Seydel, J. Phys. Chem. B **126**, 7400 (2022).
[51] D. J. Jeffrey and Y. Onishi, Z. Angew. Math. Phys. **35**, 634 (1984).
[52] A. K. Townsend, "The mechanics of suspensions," Ph.D. thesis, UCL (University College London), 2017.
[53] G. H. Koenderink, H. Zhang, D. G. Aarts, M. P. Lettinga, A. P. Philipse, and G. Nägele, Faraday Discuss. **123**, 335 (2003).
[54] G. Nägele, J. Phys.: Condens. Matter **15**, S407 (2003).